ORIGINAL ARTICLE

Metabonomics of human fecal extracts characterize ulcerative colitis, Crohn's disease and healthy individuals

Jacob Tveiten Bjerrum · Yulan Wang ·
Fuhua Hao · Mehmet Coskun · Christian Ludwig ·
Ulrich Günther · Ole Haagen Nielsen

Abstract This study employs spectroscopy-based metabolic profiling of fecal extracts from healthy subjects and patients with active or inactive ulcerative colitis (UC) and Crohn's disease (CD) to substantiate the potential use of spectroscopy as a non-invasive diagnostic tool and to characterize the fecal metabolome in inflammatory bowel disease (IBD). Stool samples from 113 individuals (UC 48, CD 44, controls 21) were analyzed by ^{1}H nuclear magnetic resonance (NMR) spectroscopy (Bruker 600 MHz, Bruker BioSpin, Rheinstetten, Germany). Data were analyzed with principal component analysis and orthogonal-projection to latent structure-discriminant analysis using SIMCA-P + 12 and MATLAB. Significant differences were found in the metabolic profiles making it possible to differentiate between active IBD and controls and between UC and CD. The metabolites holding differential power primarily belonged to a range of amino acids, microbiota-related short chain fatty acids, and lactate suggestive of an inflammation-driven malabsorption and dysbiosis of the normal bacterial ecology. However, removal of patients with intestinal surgery and anti-TNF-α antibody treatment eliminated the discriminative power regarding UC versus CD. This study consequently demonstrates that ^{1}H NMR spectroscopy of fecal extracts is a potential non-invasive diagnostic tool and able to characterize the inflammation-driven changes in the metabolic profiles related to malabsorption and dysbiosis. Intestinal surgery and medication are to be accounted for in future studies, as it seems to be factors of importance in the discriminative process.

J. T. Bjerrum
Department of Cellular and Molecular Medicine, The Panum Institute, University of Copenhagen, Copenhagen, Denmark
e-mail: bjerrum.jacob@gmail.com

J. T. Bjerrum · M. Coskun · O. H. Nielsen
Department of Gastroenterology, Medical Section, Herlev Hospital, University of Copenhagen, Copenhagen, Denmark

Y. Wang (✉) · F. Hao
Key Laboratory of Magnetic Resonance in Biological Systems, State Key Laboratory of Magnetic Resonance and Atomic and Molecular Physics, Wuhan Centre for Magnetic Resonance, Wuhan Institute of Physics and Mathematics, The Chinese Academy of Sciences, Wuhan, People's Republic of China
e-mail: yulan.wang@wipm.ac.cn

Y. Wang
Collaborative Innovation Center for Diagnosis and Treatment of Infectious Diseases, Hangzhou, People's Republic of China

C. Ludwig · U. Günther
HWB-NMR, School of Cancer Sciences, University of Birmingham, Edgbaston, Birmingham, UK

Keywords Diagnostic tool · Dysbiosis · Inflammatory bowel disease · Metabolomics · NMR spectroscopy

Abbreviations

ANOVA	Analysis of variance
AUC	Area under the curve
BCAA	Branched chain amino acid
CD	Crohn's disease
CPMG	Carr-Purcell-Meiboom-Gill
CV-ANOVA	Analysis of variance of the cross-validated residuals
HB	Harvey-Bradshaw
IBD	Inflammatory bowel disease
IBDU	Inflammatory bowel disease unclassified
MS	Mass spectrometry
NMR	Nuclear magnetic resonance

O-PLS-DA	Orthogonal partial least squares-discriminant analysis
PCA	Principal component analysis
PLS-DA	Partial least squares-discriminant analysis
ROC	Receiver operating characteristic
SCFA	Short chain fatty acid
TNF	Tumor necrosis factor
UC	Ulcerative colitis
UV	Unit variance

1 Introduction

Ulcerative colitis (UC) and Crohn's disease (CD) are the two main entities under the umbrella diagnosis of chronic inflammatory bowel disease (IBD). These two similar, yet distinct diseases are believed to be the consequence of an unbalanced immunological response towards intestinal microbes or components hereof in genetically predisposed individuals (Baumgart and Sandborn 2012; Ordás et al. 2012). However, despite of our current knowledge and understanding, the etiology and exact pathophysiology largely remain unknown. The diagnostics of IBD is based on a multidisciplinary approach (clinical history, endoscopy, radiology, histology, microbiology, and hematology), which is disadvantaged by its invasive nature, its time consuming procedures, and the fact that it leaves ∼10 % of the patients with the diagnosis of "IBD unclassified" (IBDU) (Geboes et al. 2008). The diagnostic delay (Vavricka et al. 2012) and lack of differential power (i.e. IBDU) imposes serious clinical implications, as early and correct diagnosis is important both for the patients' quality of life as well as for a successful clinical management (Etchevers et al. 2008; Ricart et al. 2008).

New technologies have recently been put into play and as a consequence transcriptomics (Bjerrum et al. 2010a; Olsen et al. 2009; Sipos et al. 2011; von Stein et al. 2008; Wu et al. 2007; Bjerrum et al. 2013; Planell et al. 2013), metabonomics, (Bjerrum et al. 2010b; Balasubramanian et al. 2009; Schicho et al. 2012; Williams et al. 2012; Bezabeh et al. 2001; Bjerrum et al. 2008; Zhang et al. 2013; Ooi et al. 2011) and integration of omics (Bjerrum et al. 2014) have produced promising results with respect to refinement and improvement of the diagnostics and understanding of the pathophysiology of IBD. The drawback is, however, that the majority of these studies are based on sample types acquired via invasive or semi-invasive procedures (e.g. endoscopic pinch biopsies, surgically removed colonic tissue, or blood). Non-invasive tests are badly needed for the diagnostics and the surveillance of the disease activity. Such tests would provide a higher degree of compliance in this patient population and ultimately it might lead to a better disease control for the individual patient with IBD.

With the intention to identify metabolic biomarkers and explore the possibilities of developing non-invasive tests, metabonomics studies have used urine samples from experimental animal IBD models (Murdoch et al. 2008; Lin et al. 2009; Dong et al. 2013; Schicho et al. 2010; Tso et al. 2013) and IBD patients (Williams et al. 2009; Schicho et al. 2012; Bjerrum et al. 2010b; Stephens et al. 2012; Dawiskiba et al. 2014) as an easily collected and handled sample type. The results so far have been promising but also conflicting. By contrast, it is well known that the gut microbiota differs between CD, UC, and controls (Sartor 2008), and as a consequence the preliminary metabonomics studies (Marchesi et al. 2007; Jansson et al. 2009; Le Gall et al. 2011; Walton et al. 2013) using metabolic profiles of fecal extracts have consistently been able to differentiate between IBD and controls as well as between IBD subtypes.

These promising preliminary results—together with the much needed non-invasive tests—animated the initiation of the current study in which we aimed to employ ^{1}H nuclear magnetic resonance (NMR) spectroscopy-based metabolic profiling of fecal extracts from healthy subjects and patients with active or inactive UC and CD. This was performed to substantiate the potential use of ^{1}H NMR spectroscopy as a non-invasive diagnostic tool and to characterize the fecal metabolome in IBD.

2 Materials and methods

2.1 Patient population

All patients participated in this study in confirmation with the principals outlined in the Declaration of Helsinki and with the approval of the Scientific Ethics Committee of the Copenhagen Capital Region (22 054/H-C-2009-037). Informed written consent was obtained from each participating person.

Patients were recruited at the Department of Gastroenterology, Medical Section, Herlev Hospital, Denmark. All eligible UC (n = 48) and CD (n = 44) patients subsequently had their diagnosis verified by well-established criteria (Nikolaus and Schreiber 2007) and were at the time of enrolment graded in accordance with the Mayo-score (Schroeder et al. 1987) (a score of 0–1 inactive UC, 2–4 mild UC, 5–8 moderate UC, and 9–12 severe UC) or Harvey-Bradshaw-score (Harvey and Bradshaw 1980) (a HB-score score of 0–4 inactive CD, 5–8 mild CD, 9–16 moderate CD, and >16 severe CD). See Table 1 for clinical details.

Table 1 Clinical details

Characteristics	Inactive CD n = 31	Active CD n = 13	Inactive UC n = 29	Active UC n = 19	Controls n = 21
Gender (male/female)	13/18	6/7	14/15	11/8	13/8
Age, years (mean, range)	44 (18–80)	36 (22–57)	48 (27–72)	48 (25–80)	40 (18–73)
Age at diagnosis (≤25/>25 years)	10/21	8/5	5/24	3/16	–
Years with disease (≤10/>10 years)	16/15	9/4	12/17	14/5	–
HB-score (mean, range)	1 (0–4)	10 (5–18)	–	–	–
Mayo-score (mean, range)	–	–	0.3 (0–1)	7 (3–11)	–
Extension (P/PS/LC/PC/Ileit)	–	2/2/3/1/9	–	1/2/4/11/0	–
Surgery (IR/IR+HC/HC/C)	6/2/2/3	3/2/1/1	0/0/1/2	0/0/0/0	–
Smoking/non-smoking	9/22	5/8	7/22	2/17	2/19
EIM (present/not present)	6/25	1/12	1/28	1/18	–
Steroids, n					
Responder/non-responder/unknown	24/0/7	9/3/1	17/2/10	14/3/2	–
Independent/dependent/unknown	21/3/7	4/8/1	17/2/10	10/7/2	–
Daily medication, n					
Sulfasalazine (1.5–2.0 g)	1	0	2	1	–
Systemic 5-aminosalicylic acid (1.6–3.2 g)	2	0	24	17	–
Topical 5-aminosalicylic acid (1 g)	0	0	5	11	–
Systemic glucocorticoids (75 mg)	1[a]	4	2[a]	10	–
Topical glucocorticoids (100 mg)	0	1	1	3	–
Azathioprine (100–150 mg)	9	3	2	0	–
6-Mercaptopurine (50–75 mg)	1	0	1	0	–
Infliximab (5 mg/kg)	3	4	1	0	–
None	17	3	2	0	21

CD Crohn's disease; *EIM* extraintestinal manifestations; *HB* Harvey-Bradshaw score; *UC* ulcerative colitis; *P* proctitis; *PS* proctosigmoiditis; *LC* left-sided colitis; *PC* pancolitis; *IR* Ileocaecal resection; *HC* hemicolectomia; *C* colectomia

[a] Dose of 5 mg/day

The healthy volunteers (n = 21) were recruited locally among the staff at Herlev Hospital—in all 113 individuals were included. Exclusion criteria were age above 80 or below 18 years, clinical evidence of infection, recent (within 14 days) use of antibiotics or probiotics, pregnancy, severe mental illness and special food regimens such as FODMAP, diabetic diets, and gluten-free diet.

2.2 Sample collection and preparation

Each participant was given a sample collection kit with instructions. Hence, one fecal sample from each subject was collected, placed in a sealed insulate container, immediately put on ice, and subsequently delivered to the laboratory within 3 h, where it was stored at −80 °C. Previous experiments (Bezabeh et al. 2009) using un-extracted raw samples produced spectra with a poor resolution, whereas Marchesi et al. (2007) and Jacobs et al. (2008) achieved excellent results with water extracts and a pH above 7. Hence, fecal water was extracted by taking a weighed sample of thawed stool material

and adding 2 volumes (w/v) of sterile phosphate buffered saline (PBS 1.9 mM Na_2HPO_4, 8.1 mM NaH_2PO_4, 150 mM NaCl, pH 7.4). The mixture was homogenized by vortexing vigorously for 1 min. The fecal slurry was centrifuged at $3,000 \times g$ for 15 min, and the supernatant was filtered through a syringe with a needle (0.40×25 mm). The filtrate was centrifuged at $14,000 \times g$ for 30 min, and the supernatant filtered through a Whatman 25 mm GD/X PES sterile syringe filter (pore size 0.2 μm). The filtered fecal water was stored at −80 °C until subsequent analysis.

The fecal extracts were finally prepared by mixing 4 μl of D_2O/500 μM TSP (3-trimethylsilyl-2,2,3,3-tetradeuterosodium propionate, final TSP = 50 μM) with 40 μl of fecal extract in a 96-hole shallow hole plate. A total of 35 μl from each of these mixed samples were transferred into 1.7 mm outer diameter NMR tubes in a SampleJet rack used for the NMR experiments. Previous investigations on fecal extracts have shown no marked changes in the resonances of interest as a result of the freeze/thawing cycle (Bezabeh et al. 2009; Saric et al. 2008).

2.3 ^{1}H NMR spectroscopy

All ^{1}H NMR experiments were performed at 288.1 K, using a Bruker 600 MHz spectrometer operating at 600.13 MHz for proton and equipped with an inverse detection cryogenic probe (BrukerBioSpin, Rheinstetten, Germany). For all samples, the ^{1}H NMR spectra were acquired using a CPMG (Carr-Purcell-Meiboom-Gill) pulse sequence with an echo-time of 160 ms. The 90° pulse length was approximately 10 µs as calculated automatically for each sample. A total of 256 scans were collected into 32 k data points with a spectral width of 12 ppm. NMR resonances were assigned according to previous published data (Marchesi et al. 2007).

2.4 Data analysis

The free induction decays for one-dimensional data were zero-filled to 64 k data points and multiplied by an exponential function with a line-broadening factor of 0.5 Hz prior to Fourier transformation. All one-dimensional ^{1}H NMR spectra were manually corrected for phase and baseline distortions using TOPSPIN 2.1(BrukerBiospin) and referenced to the TSP signal at δ 0.0 ppm. ^{1}H NMR spectral regions δ 0.5–9.0 were binned with a width of 0.004 ppm (2 Hz) using the AMIX package (v3.9.3, BrukerBiospin). Water regions δ 4.4–5.2 were removed in order to avoid imperfect water saturation. Additionally, all UC patients were treated with 5-aminosalicylic acid; hence the resonances from 5-aminosalicylic acid and its metabolite, N-acetyl-5-aminosalicylic acid, which include the entire aromatic region and δ 2.12–2.26, were removed whenever group comparisons involved UC patients. For the comparisons between CD and controls, two samples contained 5-aminosalicylic acid and N-acetyl-5-aminosalicylic acid and these samples were excluded from the analysis. The decision to exclude the two CD samples and thus keep the aromatic region in the remaining CD samples, as opposed to the UC samples, is based on the principle of keeping as many data as possible in order to generate valid results.

The ^{1}H NMR spectra were normalized to the total sum of the spectral integrals to compensate for sample concentration differences. Subsequently, the multivariate data analyses were carried out using the SIMCA-P + software package (v12.0, Umetrics, Umeå, Sweden). Initially, the principal component analysis (PCA) of the ^{1}H NMR spectral data was performed (on mean-centered data) to visualize the general structure of each data set and to identify any abnormalities (based on the principles of Hotelling T^2) within the data set. Next, the supervised multivariate methods, projection to latent structure-discriminant analysis (PLS-DA) and orthogonal-projection to latent structure-discriminant analysis (O-PLS-DA)

(Bylesjö et al. 2006) was applied to the analysis of ^{1}H NMR spectral data scaled to unit variance (UV) in order to uncover metabolic differences. O-PLS is an extension of the partial least square regression method featuring an integrated orthogonal signal correction filter (Trygg and Wold 2002). The interpretation of the model is facilitated by a back-scaled transformation of the loadings, with incorporated color-coded correlation coefficients (MAT-LAB v7.1, The MathWorks Inc, Natick, MA, USA) of the metabolites responsible for the differentiation as described by Cloarec et al. (2005). In short, each back-scaled loading is plotted as a function of the respective chemical shift with a color code that indicates the weights of the discriminatory variables. A hot color (red) corresponds to the metabolite being markedly different between classes, while a cool color (blue) corresponds to no differences between classes.

In order to validate and avoid the risk of over-fitting the PLS model, a sevenfold cross-validation was used, i.e. iterative construction of models by repeatedly leaving out one-seventh of the samples, and predicting them back into the model. This procedure results in a cross-validation parameter Q^2, indicating the predictability of the model in relation to its statistical validity. An additional cross-validation tool, a permutation test, was performed for each model: 200 models were constructed with the use of randomized classification for the samples and Q^2 generated from these models were compared to the Q^2 of the real model. If the maximum value of Q^2_{max} from the permutation test was smaller than the Q^2 of the real model, the model was regarded as a predictable model. Similarly, the R^2 was used to evaluate possibly over-fitted models. A final significance test was performed with the use of a CV-ANOVA (analysis of variance of the cross-validated residuals) (Eriksson et al. 2008) test to verify the models validity. The models were only considered to be valid if the permutation test and the CV-ANOVA test were satisfied at the same time.

In order to determine the sensitivity and specificity of the established models receiver operating characteristic curves (ROC) of true positive rates were plotted as a function of false positive rates in SPSS using cross-validated Y prediction values. The subsequent areas of under the ROC curves were also calculated in SPSS.

3 Results

3.1 ^{1}H NMR spectra of fecal extracts

Typical ^{1}H NMR spectra of fecal extracts obtained from controls and active and inactive CD and UC patients are shown in supplementary material 1. A range of endogenous metabolites observed in the spectra are similar to

Table 2 Validation of PLS-DA and O-PLS-DA models

	CV-ANOVA (p-value)	Permutation (n = 200)
A) Models		
Active UC vs. inactive UC	0.0160 √	X
Active UC vs. controls	*0.0006 √*	√
Inactive UC vs. controls	0.0297 √	X
Active UC vs. active CD	0.1083 X	X
Inactive UC vs. inactive CD	*0.0018 √*	√
Active CD vs. inactive CD	0.2101 X	X
Active CD vs. controls	*0.0009 √*	√
Inactive CD vs. controls	*0.0035 √*	√
B) Models corrected for pouch/ileostomy		
Active UC vs. inactive UC	*0.0013 √*	√
Active UC vs. controls	*0.0006 √*	√
Inactive UC vs. controls	0.0065 √	X
Active UC vs. active CD	0.0973 X	X
Inactive UC vs. inactive CD	*0.0001 √*	√
Active CD vs. inactive CD	1.0000 X	X
Active CD vs. controls	*0.0045 √*	√
Inactive CD vs. controls	0.0191 √	X
C) Models corrected for intestinal surgery		
Active UC vs. inactive UC	*0.002 √*	√
Active UC vs. controls	*0.000 √*	√
Inactive UC vs. controls	0.013 √	X
Active UC vs. active CD	0.698 X	X
Inactive UC vs. inactive CD	0.317 X	X
Active CD vs. inactive CD	0.287 X	X
Active CD vs. controls	1.000 X	X
Inactive CD vs. controls	0.128 X	X

The models were only considered valid if the permutation test and the CV-ANOVA test ($p < 0.05$) were satisfied at the same time—italicized text

A) The models are based on all samples except for 10 excluded samples: 9 outliers of which 2 had an ileostomy and 4 had segmental surgery, and the three remaining outliers could not be connected to any clinical demographics. The last excluded sample was due to overlapping drug metabolites. Remaining number of patients: inactive UC: n = 25, active CD: n = 11, inactive UC: n = 27, active UC: n = 19, controls: n = 21

B) The models are based on all samples except for 11 excluded samples: 7 IBD patients with an ileostomy, 1 inactive UC patient with a pouch, and 3 outliers. Remaining number of patients: inactive UC: n = 25, active CD: n = 11, inactive UC: n = 25, active UC: n = 19, controls: n = 21

C) The models are based on all samples except for 25 excluded samples: 23 IBD patients with any kind of intestinal surgery and 2 outliers. Remaining number of patients: inactive UC: n = 17, active CD: n = 6, inactive UC: n = 25, active UC: n = 19, controls: n = 21

CD Crohn's disease, *CV-ANOVA* analysis of variance of the cross-validated residuals, *O-PLS-DA* orthogonal-projection to latent structure-discriminant analysis, *UC* ulcerative colitis

√ valid model

X invalid model

previously detected metabolites (Le Gall et al. 2011; Jansson et al. 2009; Marchesi et al. 2007), and include a number of amino acids, such as leucine, isoleucine, valine, lysine, alanine, tyrosine, phenylalanine, glycine, glutamate, and aspartate, and the microbiota-related metabolites including butyrate, propionate, and lactate. Furthermore, the exogenous metabolites 5-aminosalicylic acid and *N*-acetyl-5-aminosalicylic acid were detected in the samples from UC patients and in two CD samples, and originated from the medication Mesalazine taken by all of the UC patients and two CD patients (Table 1). Subsequent analyses indicated that formate, fumerate, phenylalanine, and tyrosine were all present in the excluded regions.

Fig. 1 OPLS-DA score plots. The score plots (**a**, **b**, **c**, and **d**) are based on the four valid models containing all patients and display the 1st PLS component and one orthogonal component for each model. A two-way separation of the fecal samples is demonstrated in all 4 plots. *Blue diamonds* control; *empty triangles* active CD; *red dots* inactive CD; *empty circles* active UC; *purple stars*: inactive UC. The corresponding *back-scaled* loading plots reflect the class differences in the NMR spectra. *Upright peaks* indicate a relatively increased intensity of metabolites, and *downright peaks* a decreased intensity of metabolites. The *colors* shown on the plot are associated with the significance of metabolites in separating the samples as shown on the *right hand side of the plot*, where the *color-scaling map* is given together with the respective correlation coefficients. In accordance with the sample number in each group and a significance level of p < 0.05, the metabolites are significant at correlation coefficient values above **a** 0.55, **b** 0.43, **c** 0.44, and **d** 0.38, respectively. *CD* Crohn's disease; *UC* ulcerative colitis; *ala* alanine; *asp* aspartate; *buty* butyrate; *glu* glutamate; *gly* glycine; *ileu* isoleucine; *lac* lactate; *leu* leucine; *lys* lysine; *phe* phenylalanine; *prop* proprionate; *tyr* tyrosine; *val* valine (Color figure online)

OPLS-DA score plots (left) and corresponding loading plots (right)
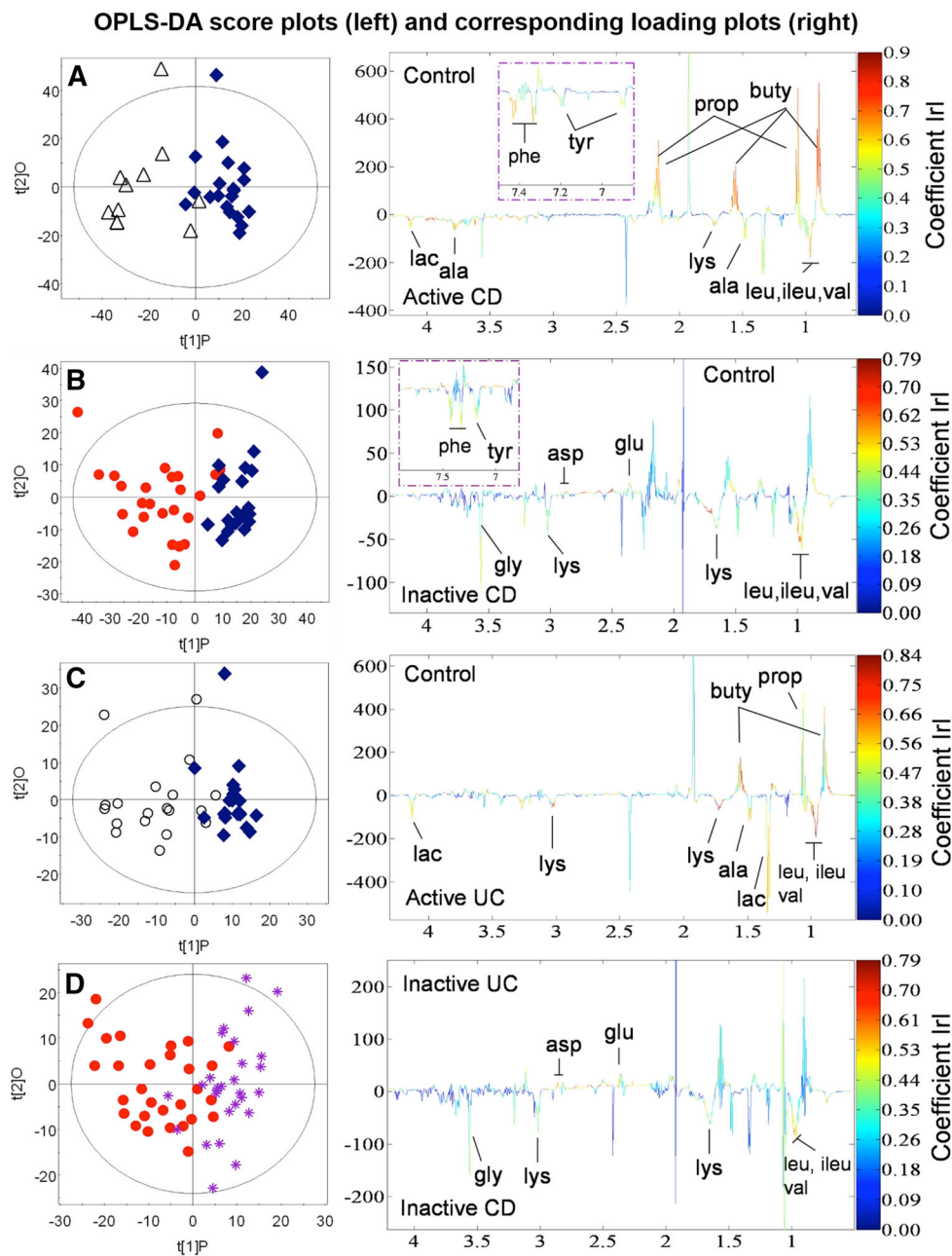
3.2 Multivariate data analysis of ^{1}H NMR spectra

PCA was initially applied to the NMR spectra acquired from the fecal extracts using data scaled to UV. Based on the principals of Hotelling T^2 (95 % confidence limit) a total number of 9 samples had to be removed (2 had an ileostomy, 4 had segmental surgery, and 3 could not be connected to any clinical demographics) and one sample was excluded due to overlapping drug metabolites, in all 10 samples were excluded.

In order to classify the samples PLS-DA models comparing controls with active and inactive UC and CD,

respectively, UC and CD (i.e. active UC vs. active CD, inactive UC vs. inactive CD), and different disease states (i.e. active UC vs. inactive UC and active CD vs. inactive CD) were generated; CPMG NMR data as an X matrix and class information as the Y variables (Cloarec et al. 2005), i.e. control, active UC, inactive UC, active CD, and inactive CD. To uncover the metabolic changes holding differential power, the O-PLS-DA strategy was subsequently applied to each model. The O-PLS-DA models were constructed with one PLS component and one orthogonal component for each model. Each model was subsequently validated with the use of a permutation test (for the PLS-

DA models, see supplementary material 2) and a CV-ANOVA (for the O-PLS-DA models).

As seen in Table 2A four of the models met the validation requirements when the data analyses were performed on all five groups. However, 6 of the 10 excluded samples originated from patients having had intestinal surgery, indicating that surgery might have a significant impact on the fecal metabolome. Predictive models, i.e. PLS-DA and O-PLS-DA, were consequently generated in order to further characterize the impact of different surgical interventions. Patients who had a colectomy were identified and removed from the analysis: one patient had a pouch (inactive UC) and seven patients had an ileostomy (4 inactive CD, 2 active CD, and 1 inactive UC) of which only two patients received TNF-α inhibitor treatment (1 inactive CD and 1 active CD). Removing these 8 samples resulted in the model comparing control with inactive CD becoming invalid, whereas the model comparing inactive UC with active UC became valid, Table 2B. Subsequent removal of the remaining patients (coincides with removal of all 8 patients receiving anti-TNF-α antibody treatment), who also had intestinal surgery, but maintain a continuous gastrointestinal tract with a partially preserved colon, resulted in further drastic changes in the predictive models: inactive UC vs. inactive CD and active CD vs. controls also became invalid. Only two models met the final validation requirements, Table 2C. The corresponding score-plots and their back-scaled loading plots are shown in Fig. 1 (all samples) and Fig. 2 (samples from patients with intestinal surgery excluded), where a clear separation between each class is seen in the score-plots. The corresponding back-scaled loading plots reflect the class differences of the NMR spectra and indicate relatively increased or decreased intensities of metabolites. These back-scaled loading plots were converted into comprehensive lists of markedly up- and down-regulated metabolites in Table 3 (3A all patients included and 3B intestinal surgery patients excluded). The significant metabolites proposed from the correlation coefficients were further validated and compared with the use of a simple Student's t test and by ANOVA and subsequently corrected for multiple testing using Bonferroni and Tamhane, respectively (Table 3). The actual prediction performance estimates are presented in Table 4 as area under the curve (AUC) and correlates with the results of the OPLS-DA models; only the models active UC vs. inactive UC and active UC vs. controls demonstrate AUC >80. The AUCs are presented in supplementary material 3.

Furthermore, predictive models were generated within each disease phenotype (inactive CD, active CD, and inactive UC) comparing patients with and without intestinal resection. However, none of these models were predictive (data not included). A similarly approach was applied to the group of inactive CD patients; 17 of these were medication free, thus providing an opportunity to elucidate on the potential effect of medication on the fecal metabolome. The group of inactive CD patients was accordingly sub-divided into four classes: (1) without surgery and no medication (n = 10), (2) without surgery but on medication (n = 8), (3) with surgery but no medication (n = 7), and (4) with surgery and on medication (n = 6). These four classes were as previously described compared with predictive modeling, but none of them turned out to be valid, although a trend (p = 0.14) was observed between class 1 and 4 (supplementary material 4).

A final analysis was performed on the different sub-phenotypes: gender, age at diagnosis ($\leq$25 years/ >25 years), years with diagnosis ($\leq$10 years/>10 years), Mayo-score and HB-score (mild, moderate, and severe), extent of inflammation (proctitis, proctosigmoiditis, left-sided colitis, pancolitis, and ileitis), smoking status (smoking/non-smoking), extra-intestinal manifestations (present/not present), and steroids (responder/non-responder and dependent/non-dependent). This was completed by creating PLS-DA models for each patient category; NMR data as an X matrix and phenotype information as the Y variables. None of the models, however, turned out to be predictive (data not included).

4 Discussion

With the use of ^{1}H NMR spectroscopy-based metabonomics and fecal extracts from a large cohort of IBD patients, the current study demonstrates both the possibilities and limitations held by this technique as a diagnostic tool in terms of discriminating between UC, CD, and controls.

A recent study (Stephens et al. 2012) on urinary metabolic profiles of IBD patients and healthy controls has documented the importance of identifying confounding factors such as medication and intestinal surgery when using an NMR spectroscopy-based approach. Similar results are presented in the current study, as CD and UC patients can be distinguished from the control group (Table 2A), but exclusion of the 8 patients who had a total colectomy created drastic changes in the predictive results (Table 2B). Further significant changes in the predictive abilities were also identified with subsequent removal of patients, who only had segmental intestinal surgery performed and a preserved continuous gastrointestinal tract. Thus, removing all patients with intestinal surgery, which coincides with the elimination of all 8 patients receiving TNF-α inhibitor treatment, leaves only two valid models: active UC vs. inactive UC and active UC vs. controls (Tables 2C and 4). In this context, it is important to note that even minor intestinal surgery, i.e. segmental resection,
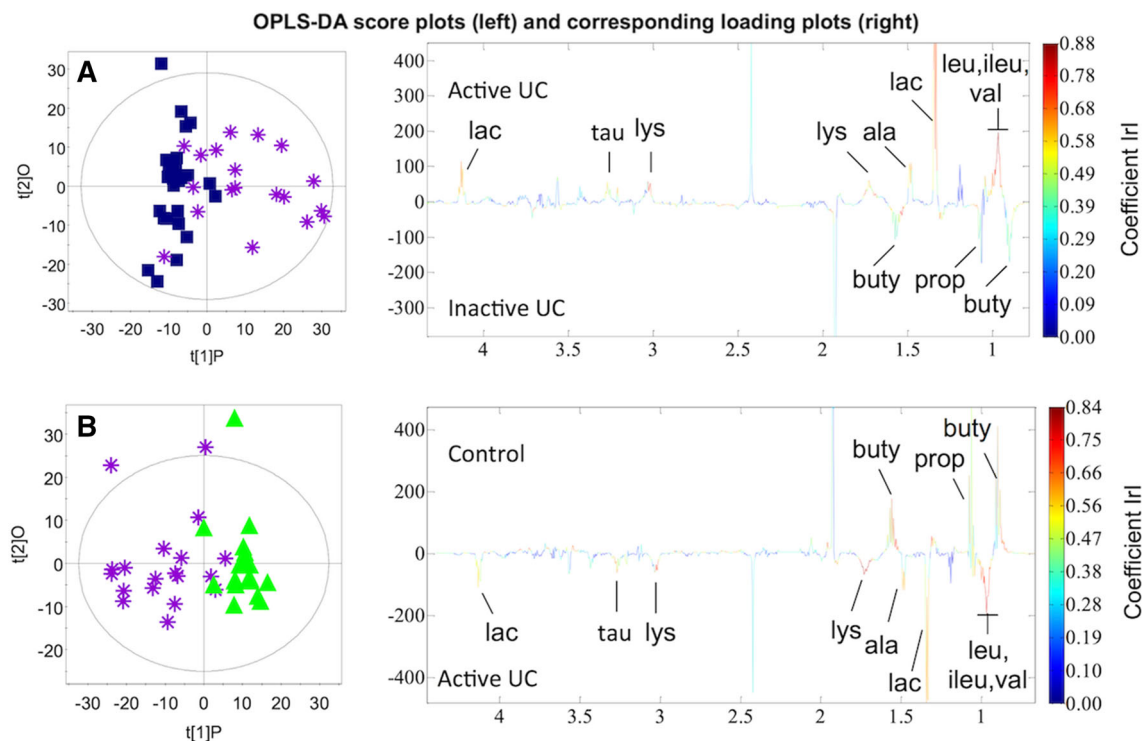
Fig. 2 OPLS-DA score plots of patients without intestinal surgery. The score plots (**a** and **b**) are based on the two valid models containing only patients without intestinal surgery and display the 1st PLS component and one orthogonal component for each model. A two-way separation of the fecal samples is demonstrated in both plots. *Blue squares* inactive UC; *purple stars* active UC; *green triangles* controls. The corresponding back-scaled loading plots reflect the class differences in the NMR spectra. *Upright peaks* indicate a relatively increased intensity of metabolites, and downright peaks a decreased intensity of metabolites. The *colors* shown on the plot are associated with the significance of metabolites in separating the samples as shown on the *right hand side* of the plot, where the *color-scaling map* is given together with the respective correlation coefficients in accordance with the sample number in each group and a significance level of p < 0.05, the metabolites are significant at correlation coefficient values above **a** 0.44 and **b** 0.44, respectively. *UC* ulcerative colitis; *ala* alanine; *buty* butyrate; *ileu* isoleucine; *lac* lactate; *leu* leucine; *lys* lysine; *prop* proprionate; *tau* taurine; *val* valine (Color figure online)

seems to have a significant impact on the fecal metabolome.

To further elaborate on the effect of surgery and medication subsequent predictive models of surgery versus no surgery within each disease phenotype, i.e. inactive CD, active CD, and inactive UC, and between different sub-classes of inactive CD (supplementary material 4) were created. Surprisingly, none of these models were valid. This either indicates that an even larger cohort of patients is needed to improve the differential power or signifies an inherent weakness in the current approach: overlapping drug resonances, which often leads to the exclusion of large spectral regions and thus potential vital metabolites holding differential power—or both. Formate, fumerate, phenylalanine, and tyrosine were identified in the excluded spectral regions in the current study as potential informative and predictive metabolites.

Recent studies have characterized the fecal metabolome of different gastrointestinal disorders such as IBD, IBS and colorectal cancer using mass spectrometry (MS) usually combined with gas or liquid chromatography (Ahmed et al. 2013; Garner et al. 2007; Duboc et al. 2013). MS generally exhibits better sensitivity, selectivity and a broader dynamic range compared to NMR, but often requires pre-treatment of the samples introducing additional sources of variability to the metabonomics data. Thus, to overcome problems with overlapping drug resonances and generally improve the metabonomics data a combination of different analytical technologies, e.g. NMR and MS, is needed so as to obtain a better coverage of the metabolites and differential power.

The results of the current study are in contrast to Marchesi et al. (2007) who used the exact same methodology and were able to differentiate not only between active IBD and controls, but also between active CD and active UC. The metabolites holding differential power in the Marchesi study (active CD vs. active UC) were primarily branched chain amino acids (BCAA; isoleucine, leucine, and valine) found in greater abundance in CD samples. The present study also found greater abundance of BCAA and a range

Table 3 Changed metabolites in the valid models

A)

Metabolites	Active CD/controls $Q^2 = 0.52$, r > 0.55	Student's t test (p-value)	ANOVA (p-value)	Inactive CD/controls $Q^2 = 0.32$, r > 0.43	Student's t test (p-value)	ANOVA (p-value)	Active UC/controls $Q^2 = 0.43$, r > 0.44	Student's t test (p-value)	ANOVA (p-value)	Inactive CD/inactive UC $Q^2 = 0.28$, r > 0.38	Student's t test (p-value)	ANOVA (p-value)
ileu	↑	0.002*	0.00*	↑	0.230	1.00	↑	0.009*	0.14	↑	0.307	1.00
leu	↑	0.001*	0.01*	↑	0.013*	0.12	↑	0.000*	0.00*	↑	0.075	0.54
val	↑	0.002*	0.02*	↑	0.014*	0.14	↑	0.001*	0.01*	↑	0.056	0.44
lys	↑	0.001*	0.01*	↑	0.092	0.62	↑	0.000*	0.00*	↑	0.113	0.70
ala	↑	0.001*	0.01*	–	0.294	0.94	↑	0.003*	0.03*	–	0.878	1.00
tyr	↑	0.044*	0.12	↑	0.074	0.97	–	–	–	–	–	–
phe	↑	0.003*	0.00*	↑	0.695	0.21	–	–	–	–	–	–
gly	↑	0.034*	0.29	↑	0.042*	0.35	↓	0.016*	0.15	↑	0.111	0.69
buty	↓	0.000*	0.00*	–	0.372	0.99	↓	0.179	0.86	–	0.991	1.00
prop	↓	0.051*	0.40	–	0.201	0.89	↓	0.147	0.80	–	0.036*	0.31
lac	–	0.226	0.92	–	0.474	0.99	↑	0.044*	0.36	–	0.459	1.00
asp	–	0.064	0.57	↓	0.044*	0.36	–	0.708	0.99	↓	0.001*	0.01*
glu	–	0.307	1.00	↓	0.001*	0.06	–	0.222	1.00	↓	0.000*	0.00*

B)

Metabolites	Active UC/inactive UC $Q^2 = 0.34$, r > 0.44	Student's t test (p-value)	ANOVA (p-value)	Active UC/controls $Q^2 = 0.46$, r > 0.44	Student's t test (p-value)	ANOVA (p-value)
ileu	↑	0.016*	0.030*	↑	0.009*	0.019*
leu	↑	0.001*	0.000*	↑	0.000*	0.000*
val	↑	0.002*	0.000*	↑	0.001*	0.000*
lys	↑	0.000*	0.000*	↑	0.000*	0.000*
ala	↑	0.012*	0.007*	↑	0.003*	0.001*
buty	↓	0.526	1.000	↓	0.179	1.000
prop	↓	0.394	1.000	↓	0.147	0.946
lac	↑	0.050	0.012*	↑	0.044*	0.015*
tau	↑	0.014*	0.029*	↑	0.002*	0.002*

A) ↑ increased or ↓ decreased compared to control and inactive UC. Valid models based on all included samples

B) ↑ increased or ↓ decreased compared to inactive UC and control. Valid models based on samples from patients, who have not had intestinal surgery

Ala alanine; *asp* aspartic acid; *buty* butyrate; *gly* glycine; *glu* glutamate; *ileu* isoleucine; *lac* lactate; *leu* leucine; *lys* lysine; *phe* phenylalanine; *prop* propionate; *tau* taurine; *tyr* tyrosine; *val* valine; *ANOVA* analysis of variance; *CD* Crohn's disease; *UC* ulcerative colitis; Q^2 predictability of the model; *r* correlation coefficient

* significance (p < 0.05)

Table 4 Predictive capability of the models

Models corrected for surgery	Area under the curve	
Active UC vs. inactive UC	0.813	Good
Active UC vs. controls	0.876	Good
Inactive UC vs. controls	0.654	Poor
Active UC vs. active CD	0.693	Poor
Inactive UC vs. inactive CD	0.659	Poor
Active CD vs. inactive CD	0.529	Poor
Active CD vs. controls	0.667	Poor
Inactive CD vs. controls	0.726	Fair

Prediction performance estimates presented as area under the curve (AUC) for each model

of other amino acids (i.e. lysine, alanine, tyrosine, phenylalanine, and glycine, Table 3A) in the samples from patients with active CD and UC when compared to controls, but these metabolites were without significance when active CD and active UC were compared (Table 2A). Once corrected for surgery (and TNF-α inhibitor treatment) the higher abundance of BCAA, lysine, alanine, and taurine remained evident only for active UC compare to inactive UC and control subjects, respectively (Table 3B).

The larger amount of amino acids in active UC might very well be due to malabsorption caused by the inflammation, whereas the low levels of the short chain fatty acids (SCFAs), butyrate and propionate, seem to be the consequence of an inflammation-driven intestinal dysbiosis. Thus, a range of recent culture-independent studies repeatedly identify *Faecalibacterium prausnitzii* in lower abundance in CD (Swidsinski et al. 2009; Frank et al. 2007; Martinez-Medina et al. 2006; Sokol et al. 2008), whereas *Clostridium coccoides* has been found reduced primarily in UC (Sokol et al. 2006; Vermeiren et al. 2012). These species are important participants in the bacterial fermentation of polysaccharides and consequently the production of SCFAs. Usually SCFAs are produced in large amounts reaching millimolar concentrations in the colonic lumen from which they are absorbed (Topping and Clifton 2001). Especially butyrate is a preferred energy source for the colonocytes (Chapman et al. 1994) and exhibits, along with propionate, a well documented anti-inflammatory capacity through an inhibitory effect on TNF-α-mediated activation of the nuclear factor (NF)-κB pathway (Tedelind et al. 2007; Segain et al. 2000). Adding insult to injury, defects in butyrate transport across the epithelium and in the butyrate oxidation pathway exist during inflammation in both CD (De Preter et al. 2013) and UC (De Preter et al. 2009; Thibault et al. 2010). Thus, low levels of SCFAs seem to be the consequence of an inflammation-driven dysbiosis, but low levels of SCFAs by it self promote

sustained inflammation and thereby induce an uncontrolled spiral of chronic inflammation and dysbiosis in both CD and UC. Lactate on the other hand, is in the current study only found in greater abundance in active UC—a result that parallels previous studies (Hove et al. 1994; Vernia et al. 1988). Usually, lactate is not detected as a major fermentation product, which is assumed to reflect the presence of lactate-utilizing bacterial species in the microbiota of a healthy gut (Duncan et al. 2004). Interestingly, some of the recently identified bacterial groups of lactate-utilizing bacteria in the human gut (i.e. *E. hallii* and *A. caccae*) (Duncan et al. 2004) belong to the clostridial cluster XIVa, to which *C. coccoides* also belong. Consequently, *C. coccoides* (lower quantity in UC) might very well represent lactate-utilizing butyrate-producing bacteria, which could explain the low levels of SCFAs and greater abundance of lactate seen in active UC. In contrast, *F. prausnitzii* (lower quantity in CD) is not using lactate in its production of butyrate (Duncan et al. 2004), and no lactate increase is detected in the samples from active CD. Hence, the metabolic profiles found in the fecal samples from active UC patients consequently match the dysbiosis described by previous studies, and the results from the current study might accordingly be interpreted as a metabolic characterization of the predominant dysbiosis in active UC. However, the results in general need to be interpreted in light of potential confounding factors, such as the systemic effect of medication and changed dietary strategies during active and inactive disease, which was not accounted for in the current study.

In conclusion, ^{1}H NMR spectroscopy-based metabonomics on fecal extracts from IBD patients has proven to be a potentially powerful non-invasive diagnostic tool and able to characterize the inflammation-driven changes in the metabolic profiles related to malabsorption and a dysbiosis of the normal bacterial ecology. However, the study also highlights the fact that even minor intestinal surgery, anti-TNF-α antibody treatment, overlapping drug resonances, and medication in general are to be accounted for in future studies as these impose significant confounding factors; even though it is difficult, fecal samples need to be obtained from newly diagnosed and consequently untreated patients, and analyzed with complementary analytical technologies if we are ever to test the true potential of metabonomics as a diagnostic tool in IBD.

Conflict of interest   The authors declare no conflicts of interest.

References

Ahmed, I., Greenwood, R., de Costello, B. L., Ratcliffe, N. M., & Probert, C. S. (2013). An investigation of fecal volatile organic metabolites in irritable bowel syndrome. *PLoS One, 8*(3), e58204.

Balasubramanian, K., Kumar, S., Singh, R. R., et al. (2009). Metabolism of the colonic mucosa in patients with inflammatory bowel diseases: an in vitro proton magnetic resonance spectroscopy study. *Magnetic Resonance Imaging, 27*(1), 79–86.

Baumgart, D. C., & Sandborn, W. J. (2012). Crohn's disease. *Lancet, 380*(9853), 1590–1605.

Bezabeh, T., Somorjai, R. L., & Smith, I. C. P. (2009). MR metabolomics of fecal extracts: applications in the study of bowel diseases. *Magnetic Resonance in Chemistry, 47*(Suppl 1), S54–S61.

Bezabeh, T., Somorjai, R. L., Smith, I. C., Nikulin, A. E., Dolenko, B., & Bernstein, C. N. (2001). The use of 1H magnetic resonance spectroscopy in inflammatory bowel diseases: distinguishing ulcerative colitis from Crohn's disease. *American Journal of Gastroenterology, 96*(2), 442–448.

Bjerrum, J. T., Hansen, M., Olsen, J., & Nielsen, O. H. (2010a). Genome-wide gene expression analysis of mucosal colonic biopsies and isolated colonocytes suggests a continuous inflammatory state in the lamina propria of patients with quiescent ulcerative colitis. *Inflammatory Bowel Diseases, 16*(6), 999–1007.

Bjerrum, J. T., Nielsen, O. H., Hao, F., et al. (2010b). Metabonomics in ulcerative colitis: diagnostics, biomarker identification, and insight into the pathophysiology. *Journal of Proteome Research, 9*(2), 954–962.

Bjerrum, J. T., Nielsen, O. H., Wang, Y. L., & Olsen, J. (2008). Technology insight: metabonomics in gastroenterology-basic principles and potential clinical applications. *Nat Clin Pract Gastroenterol Hepatol, 5*(6), 332–343.

Bjerrum, J. T., Nyberg, C., Olsen, J., & Nielsen, O. H. (2013). Assessment of the validity of a multi-gene analysis in the diagnostics of inflammatory bowel disease. *Journal of Internal Medicine, 275*(5), 484–493.

Bjerrum, J. T., Rantalainen, M., Wang, Y., Olsen, J., & Nielsen, O. H. (2014). Integration of transcriptomics and metabonomics: Improving diagnostics, biomarker identification and phenotyping in ulcerative colitis. *Metabolomics, 10*, 280–290.

Bylesjö, M., Rantalainen, M., Cloarec, O., Nicholson, J. K., Holmes, E., & Trygg, J. (2006). OPLS discriminant analysis: combining the strengths of PLS-DA and SIMCA classification. *Journal of Chemometrics, 20*(8–10), 341–351.

Chapman, M. A., Grahn, M. F., Boyle, M. A., Hutton, M., Rogers, J., & Williams, N. S. (1994). Butyrate oxidation is impaired in the colonic mucosa of sufferers of quiescent ulcerative colitis. *Gut, 35*(1), 73–76.

Cloarec, O., Dumas, M. E., Trygg, J., et al. (2005). Evaluation of the orthogonal projection on latent structure model limitations caused by chemical shift variability and improved visualization of biomarker changes in 1H NMR spectroscopic metabonomic studies. *Analytical Chemistry, 77*(2), 517–526.

Dawiskiba, T., Deja, S., Mulak, A., et al. (2014). Serum and urine metabolomic fingerprinting in diagnostics of inflammatory bowel diseases. *World Journal of Gastroenterology, 20*(1), 163–174.

De Preter, V., Bulteel, V., Suenaert, P., et al. (2009). Pouchitis, similar to active ulcerative colitis, is associated with impaired butyrate oxidation by intestinal mucosa. *Inflammatory Bowel Diseases, 15*(3), 335–340.

De Preter, V., Rutgeerts, P., Schuit, F., Verbeke, K., & Arijs, I. (2013). Impaired expression of genes involved in the butyrate oxidation pathway in Crohn's disease patients. *Inflammatory Bowel Diseases, 19*(3), E43–E44.

Dong, F., Zhang, L., Hao, F., Tang, H., & Wang, Y. (2013). Systemic responses of mice to dextran sulfate sodium-induced acute ulcerative colitis using 1H NMR spectroscopy. *Journal of Proteome Research, 12*(6), 2958–2966.

Duboc, H., Rajca, S., Rainteau, D., et al. (2013). Connecting dysbiosis, bile-acid dysmetabolism and gut inflammation in inflammatory bowel diseases. *Gut, 62*(4), 531–539.

Duncan, S. H., Louis, P., & Flint, H. J. (2004). Lactate-utilizing bacteria, isolated from human feces, that produce butyrate as a major fermentation product. *Applied and Environment Microbiology, 70*(10), 5810–5817.

Eriksson, L., Trygg, J., & Wold, S. (2008). CV-ANOVA for significance testing of PLS and OPLS® models. *Journal of Chemometrics, 22*(11–12), 594–600.

Etchevers, M. J., Aceituno, M., & Sans, M. (2008). Are we giving azathioprine too late? The case for early immunomodulation in inflammatory bowel disease. *World Journal of Gastroenterology, 14*(36), 5512–5518.

Frank, D. N., St Amand, A. L., Feldman, R. A., Boedeker, E. C., Harpaz, N., & Pace, N. R. (2007). Molecular-phylogenetic characterization of microbial community imbalances in human inflammatory bowel diseases. *Proceedings of the National Academy of Sciences of the United States of America, 104*(34), 13780–13785.

Garner, C. E., Smith, S., de Lacy Costello, B., et al. (2007). Volatile organic compounds from feces and their potential for diagnosis of gastrointestinal disease. *FASEB Journal, 21*(8), 1675–1688.

Geboes, K., Colombel, J.-F., Greenstein, A., et al. (2008). Indeterminate colitis: A review of the concept—What's in a name? *Inflammatory Bowel Diseases, 14*(6), 850–857.

Harvey, R. F., & Bradshaw, J. M. (1980). A simple index of Crohn's-disease activity. *Lancet, 1*(8167), 514.

Hove, H., Nordgaard-Andersen, I., & Mortensen, P. B. (1994). Faecal DL-lactate concentration in 100 gastrointestinal patients. *Scandinavian Journal of Gastroenterology, 29*(3), 255–259.

Jacobs, D. M., Deltimple, N., van Velzen, E., et al. (2008). (1)H NMR metabolite profiling of feces as a tool to assess the impact of nutrition on the human microbiome. *NMR in Biomedicine, 21*(6), 615–626.

Jansson, J., Willing, B., Lucio, M., et al. (2009). Metabolomics reveals metabolic biomarkers of Crohn's disease. *PLoS One, 4*(7), e6386.

Le Gall, G., Noor, S. O., Ridgway, K., et al. (2011). Metabolomics of fecal extracts detects altered metabolic activity of gut microbiota in ulcerative colitis and irritable bowel syndrome. *Journal of Proteome Research, 10*(9), 4208–4218.

Lin, H.-M., Edmunds, S. I., Helsby, N. A., Ferguson, L. R., & Rowan, D. D. (2009). Nontargeted urinary metabolite profiling of a mouse model of Crohn's disease. *Journal of Proteome Research, 8*(4), 2045–2057.

Marchesi, J. R., Holmes, E., Khan, F., et al. (2007). Rapid and noninvasive metabonomic characterization of inflammatory bowel disease. *Journal of Proteome Research, 6*(2), 546–551.

Martinez-Medina, M., Aldeguer, X., Gonzalez-Huix, F., Acero, D., & Garcia-Gil, L. J. (2006). Abnormal microbiota composition in the ileocolonic mucosa of Crohn's disease patients as revealed by polymerase chain reaction-denaturing gradient gel electrophoresis. *Inflammatory Bowel Diseases, 12*(12), 1136–1145.

Murdoch, T. B., Fu, H., MacFarlane, S., Sydora, B. C., Fedorak, R. N., & Slupsky, C. M. (2008). Urinary metabolic profiles of inflammatory bowel disease in interleukin-10 gene-deficient mice. *Analytical Chemistry, 80*(14), 5524–5531.

Nikolaus, S., & Schreiber, S. (2007). Diagnostics of inflammatory bowel disease. *Gastroenterology, 133*(5), 1670–1689.

Olsen, J., Gerds, T. A., Seidelin, J. B., et al. (2009). Diagnosis of ulcerative colitis before onset of inflammation by multivariate modeling of genome-wide gene expression data. *Inflammatory Bowel Diseases, 15*(7), 1032–1038.

Ooi, M., Nishiumi, S., Yoshie, T., et al. (2011). GC/MS-based profiling of amino acids and TCA cycle-related molecules in ulcerative colitis. *Inflammation Research, 60*(9), 831–840.

Ordás, I., Eckmann, L., Talamini, M., Baumgart, D. C., & Sandborn, W. J. (2012). Ulcerative colitis. *Lancet, 380*(9853), 1606–1619.

Planell, N., Lozano, J. J., Mora-Buch, R., et al. (2013). Transcriptional analysis of the intestinal mucosa of patients with ulcerative colitis in remission reveals lasting epithelial cell alterations. *Gut, 62*(7), 967–976.

Ricart, E., García-Bosch, O., Ordás, I., & Panés, J. (2008). Are we giving biologics too late? The case for early versus late use. *World Journal of Gastroenterology, 14*(36), 5523–5527.

Saric, J., Wang, Y., Li, J., et al. (2008). Species variation in the fecal metabolome gives insight into differential gastrointestinal function. *Journal of Proteome Research, 7*(1), 352–360.

Sartor, R. B. (2008). Microbial influences in inflammatory bowel diseases. *Gastroenterology, 134*(2), 577–594.

Schicho, R., Nazyrova, A., Shaykhutdinov, R., Duggan, G., Vogel, H. J., & Storr, M. (2010). Quantitative metabolomic profiling of serum and urine in DSS-induced ulcerative colitis of mice by 1H NMR spectroscopy. *Journal of Proteome Research, 9*(12), 6265–6273.

Schicho, R., Shaykhutdinov, R., Ngo, J., et al. (2012). Quantitative metabolomic profiling of serum, plasma, and urine by (1)H NMR spectroscopy discriminates between patients with inflammatory bowel disease and healthy individuals. *Journal of Proteome Research, 11*(6), 3344–3357.

Schroeder, K. W., Tremaine, W. J., & Ilstrup, D. M. (1987). Coated oral 5-aminosalicylic acid therapy for mildly to moderately active ulcerative colitis. A randomized study. *New England Journal of Medicine, 317*(26), 1625–1629.

Segain, J. P., Raingeard de Blétière la, D., Bourreille, A., et al. (2000). Butyrate inhibits inflammatory responses through NFkappaB inhibition: implications for Crohn's disease. *Gut, 47*(3), 397–403.

Sipos, F., Galamb, O., Wichmann, B., et al. (2011). Peripheral blood based discrimination of ulcerative colitis and Crohn's disease from non-IBD colitis by genome-wide gene expression profiling. *Disease Markers, 30*(1), 1–17.

Sokol, H., Pigneur, B., Watterlot, L., et al. (2008). Faecalibacterium prausnitzii is an anti-inflammatory commensal bacterium identified by gut microbiota analysis of Crohn disease patients. *Proceedings of the National Academy of Sciences of the United States of America, 105*(43), 16731–16736.

Sokol, H., Seksik, P., Rigottier-Gois, L., et al. (2006). Specificities of the fecal microbiota in inflammatory bowel disease. *Inflammatory Bowel Diseases, 12*(2), 106–111.

Stephens, N. S., Siffledeen, J., Su, X., Murdoch, T. B., Fedorak, R. N., & Slupsky, C. M. (2012). Urinary NMR metabolomic profiles discriminate inflammatory bowel disease from healthy. *Journal of Crohn's and Colitis, 7*(2), e42–e48.

Swidsinski, A., Loening-Baucke, V., & Herber, A. (2009). Mucosal flora in Crohn's disease and ulcerative colitis - an overview. *Journal of Physiology and Pharmacology, 60*(Suppl 6), 61–71.

Tedelind, S., Westberg, F., Kjerrulf, M., & Vidal, A. (2007). Anti-inflammatory properties of the short-chain fatty acids acetate and propionate: a study with relevance to inflammatory bowel disease. *World Journal of Gastroenterology, 13*(20), 2826–2832.

Thibault, R., Blachier, F., Darcy-Vrillon, B., de Coppet, P., Bourreille, A., & Segain, J.-P. (2010). Butyrate utilization by the colonic mucosa in inflammatory bowel diseases: a transport deficiency. *Inflammatory Bowel Diseases, 16*(4), 684–695.

Topping, D. L., & Clifton, P. M. (2001). Short-chain fatty acids and human colonic function: roles of resistant starch and nonstarch polysaccharides. *Physiological Reviews, 81*(3), 1031–1064.

Trygg, J., & Wold, S. (2002). Orthogonal projections to latent structures (O-PLS). *Journal of Chemometrics, 16*(3), 119–128.

Tso, V. K., Sydora, B. C., Foshaug, R. R., et al. (2013). Metabolomic profiles are gender, disease and time specific in the interleukin-10 gene-deficient mouse model of inflammatory bowel disease. *PLoS One, 8*(7), e67654.

Vavricka, S. R., Spigaglia, S. M., Rogler, G., et al. (2012). Systematic evaluation of risk factors for diagnostic delay in inflammatory bowel disease. *Inflammatory Bowel Diseases, 18*(3), 496–505.

Vermeiren, J., Van den Abbeele, P., Laukens, D., et al. (2012). Decreased colonization of fecal Clostridium coccoides/Eubacterium rectale species from ulcerative colitis patients in an in vitro dynamic gut model with mucin environment. *FEMS Microbiology Ecology, 79*(3), 685–696.

Vernia, P., Caprilli, R., Latella, G., Barbetti, F., Magliocca, F. M., & Cittadini, M. (1988). Fecal lactate and ulcerative colitis. *Gastroenterology, 95*(6), 1564–1568.

von Stein, P., Lofberg, R., Kuznetsov, N. V., et al. (2008). Multigene analysis can discriminate between ulcerative colitis, Crohn's disease, and irritable bowel syndrome. *Gastroenterology, 134*(7), 1869–1881.

Walton, C., Fowler, D. P., Turner, C., et al. (2013). Analysis of volatile organic compounds of bacterial origin in chronic gastrointestinal diseases. *Inflammatory Bowel Diseases, 19*(10), 2069–2078.

Williams, H. R. T., Cox, I. J., Walker, D. G., et al. (2009). Characterization of inflammatory bowel disease with urinary metabolic profiling. *American Journal of Gastroenterology, 104*(6), 1435–1444.

Williams, H. R. T., Willsmore, J. D., Cox, I. J., et al. (2012). Serum metabolic profiling in inflammatory bowel disease. *Digestive Diseases and Sciences, 57*(8), 2157–2165.

Wu, F., Dassopoulos, T., Cope, L., et al. (2007). Genome-wide gene expression differences in Crohn's disease and ulcerative colitis from endoscopic pinch biopsies: insights into distinctive pathogenesis. *Inflammatory Bowel Diseases, 13*(7), 807–821.

Zhang, Y., Lin, L., Xu, Y., Lin, Y., Jin, Y., & Zheng, C. (2013). 1H NMR-based spectroscopy detects metabolic alterations in serum of patients with early-stage ulcerative colitis. *Biochemical and Biophysical Research Communications, 433*(4), 547–551.